



# University of HUDDERSFIELD

## University of Huddersfield Repository

Cross, H.E., Parkes, Gareth M.B and Brown, D.R.

Microwave calcination of Cu/Mg/Al hydrotalcite catalyst precursor

### Original Citation

Cross, H.E., Parkes, Gareth M.B and Brown, D.R. (2012) Microwave calcination of Cu/Mg/Al hydrotalcite catalyst precursor. *Applied Catalysis A: General*, 429/30. pp. 24-30. ISSN 0926860X

This version is available at <http://eprints.hud.ac.uk/id/eprint/13397/>

The University Repository is a digital collection of the research output of the University, available on Open Access. Copyright and Moral Rights for the items on this site are retained by the individual author and/or other copyright owners. Users may access full items free of charge; copies of full text items generally can be reproduced, displayed or performed and given to third parties in any format or medium for personal research or study, educational or not-for-profit purposes without prior permission or charge, provided:

- The authors, title and full bibliographic details is credited in any copy;
- A hyperlink and/or URL is included for the original metadata page; and
- The content is not changed in any way.

For more information, including our policy and submission procedure, please contact the Repository Team at: [E.mailbox@hud.ac.uk](mailto:E.mailbox@hud.ac.uk).

<http://eprints.hud.ac.uk/>

1  
2  
3  
4  
5  
6  
7  
8  
9  
10  
11  
12  
13  
14  
15  
16  
17  
18  
19  
20  
21  
22  
23

## Microwave calcination of Cu/Mg/Al hydrotalcite catalyst precursor

H. E. Cross, G. Parkes and D. R. Brown\*

*Centre for Materials and Catalysis Research, Department of Chemical and Biological Sciences, University of  
Huddersfield, Huddersfield HD1 3DH, UK.*

*d.r.brown@hud.ac.uk  
Tel 44 1484 473397 Fax 44 1484 472182*

**Keywords** Catalyst; catalysis; calcination; microwave; feedback-control; hydrotalcite; layered  
double hydroxide; mixed metal oxides; calorimetry; solid base.

1 **Abstract**

2

3 A copper-substituted hydrotalcite ( $\text{Cu}_{1.4}\text{Mg}_{4.4}\text{Al}_{2.2}(\text{CO}_3)_{1.1}(\text{OH})_{16}$ ) has been subjected to calcination  
4 under feedback-controlled microwave heating, in which microwave power is continuously modulated  
5 to generate a defined sample temperature programme or constant sample temperature. The results  
6 show that microwave calcination results in enhanced crystallinity of the resultant oxides and spinel  
7 phase formed at high temperature, compared to conventional calcination. In addition, an additional  
8 phase,  $\text{Cu}_2\text{MgO}_3$ , is detected following microwave calcination, at a bulk temperature very much lower  
9 than previously reported for copper-containing hydrotalcite. The concentrations and strengths of  
10 surface basic sites are significantly higher for materials calcined using microwaves than using  
11 conventional heating. Catalytic activities in the base-catalysed transesterification of glyceryl  
12 tributyrate with methanol are also higher. We suggest that microwave calcination under feedback-  
13 control, while allowing control of material bulk temperature during calcination and preventing major  
14 temperature excursions, may allow quite large but highly localised temperature variation, for instance  
15 as water is released during dehydroxylation, which are beneficial in developing surface defects and  
16 surface basicity.

17

18

19

20

21

## 1 **1. Introduction**

2

3 Solid materials prepared using microwave heating can yield products that differ from those generated  
4 by conventional heating, in part because different processes are induced by microwaves and also  
5 because direct heating by microwaves occurs throughout the body of a solid sample and is not  
6 restricted to the solid surface [1-7]. This is particularly important where a thermally-induced  
7 transformation results in the release of gases or vapours which have to diffuse to the surface through  
8 material which may or may not have already reacted. In these cases, different morphologies might  
9 reasonably be expected, depending on reaction gradients established between bulk and surface sites.  
10 The different heating rates under microwave heating experienced locally by, for instance, water  
11 released in a solid state transformation may also influence the nature of the ultimate products.

12

13 Despite the potential for control of surface and other properties, microwave techniques are largely  
14 unexploited for solid state processes. This is mainly because the required control of the heating  
15 process can be difficult, especially when a solid material undergoes a transformation which is  
16 accompanied by a change in the way the material couples with a microwave field. We are able to  
17 overcome this problem by using feedback-controlled microwave heating, in which the microwave  
18 power is controlled through continuous feedback from measurement of sample temperature to the  
19 microwave generator [8].

20

21 Figure 1 illustrates the value of feedback-control in a typical microwave calcination (of a copper-  
22 containing hydrotalcite). Application of a linear increase in microwave power (Fig. 1a), as an  
23 example of a heating programme with no feedback-control, results in fluctuations in sample  
24 temperature and, most importantly, temperature runaway above 450 °C. In contrast, under feedback-  
25 control (Fig. 1b) the power is varied to maintain a defined sample temperature ramp, dropping  
26 rapidly when the sample temperature reaches just over 400 °C to prevent the temperature runaway  
27 seen with no feedback-control.

28

1 *Figure 1*

2  
3 It is worth mentioning that feedback control of microwave power can also be based on the weight of  
4 the sample, adjusting power to maintain a constant rate of sample weight loss. Where a solid state  
5 reaction is taking place that involves weight loss, this method is equivalent to maintaining a constant  
6 rate of reaction through the programme. Control can also be exerted based on the partial pressure of  
7 an evolved gas [8-10].

8  
9 Layered hydrotalcite-type mixed metal hydroxides, the best known of which is based on magnesium  
10 hydroxide in which some of the metal ions are isomorphously substituted by aluminium ions, yield  
11 intimate mixtures of the oxides of the metals on calcination. These materials tend to have relatively  
12 high surface areas and they frequently show high catalytic activities, most commonly as solid bases  
13 .[11-15] The basicity can be tuned and other catalytic properties can be imparted through the  
14 incorporation of a range of catalytically active, usually divalent, metals in the brucite lattice structure  
15 [15-20]. Conventional hydrotalcites tend to show little catalytic activity in their original form but  
16 calcination yields solid mixed oxides which are, most often, Lewis bases. Brönsted basicity can be  
17 generated in the original hydrotalcite by exchange of the interlayer carbonate ions for hydroxide ions  
18 [15]. The basic properties of hydrotalcites also result in their application as adsorbents for pollutants  
19 such as NO<sub>x</sub> and SO<sub>x</sub> [21-23].

20  
21 The calcination of hydrotalcite by conventional methods has been studied in detail [24-26].  
22 Progressive temperature increase results in the loss of physically bound water and water in the  
23 interlayer regions, followed by desorption of water coordinating exchangeable anions. If carbonate  
24 anions are present, they decompose above 300 °C, although it is thought that this process may not be  
25 absolutely complete until the calcination temperature reaches 700 °C or even 800 °C [26]. The last  
26 major process is the dehydroxylation of the crystalline matrix to generate the oxides, at 400-500 °C.  
27 This is characterised by the appearance of broad lines in the X-ray diffraction pattern associated with  
28 the oxides, indicative of small crystallites. Raising the temperature further results in sintering of the

1 oxides and the formation of spinel phases. This is usually associated with a reduction in solid base  
2 catalytic activity [16]. When transition metals are isomorphously substituted for magnesium or  
3 aluminium, additional processes can occur on calcination, including reduction of the oxides to the  
4 corresponding metals at high temperature [25, 27].

5

6 Conventional heating techniques under feedback-control have previously been applied to hydrotalcite-  
7 type materials [28,29]. This earlier work is significant in that it demonstrates how feedback-control  
8 methods can be used to effectively resolve the processes leading to the loss of loosely bound water,  
9 dehydroxylation of the lattice and decomposition of interlayer carbonate ions, in a way not normally  
10 possible. So far these techniques have not been applied to microwave calcination of hydrotalcites.  
11 There is some reported work on the use of microwaves for hydrotalcite calcination, but crucially it has  
12 been without precise temperature control [30]. And since hydrotalcite calcination involves major  
13 changes in the way the solid couples with microwaves (as water is lost), temperature runaway is  
14 possible. It has to be accepted that temperatures achieved with uncontrolled microwave heating are  
15 unpredictable. Looking more widely at microwave calcination processes, it is worth pointing out that  
16 other methods have been used to exert at least some control over the temperature of the solid. In the  
17 synthesis of ceramics for example, microwaves have frequently been used to induce solid state  
18 transformations using an inert support matrix to moderate temperature excursions [31], but it is  
19 important to note that this does not provide the level of control available through continuous feedback  
20 methods.

21

22 In the work reported here we have studied the effects of microwave calcination of copper-containing  
23 layered hydroxides on the structural and catalytic properties of the mixed metal oxides produced.  
24 The work is based on a layered metal hydroxide containing aluminium, magnesium and copper(II)  
25 ions. Microwave calcination has been carried out using an indigenously developed feedback-control  
26 system, based on a tuned microwave cavity in which the sample is held at the anti-node of the  
27 fundamental stationary wave, itself produced by a variable power supply controlled by feedback from  
28 a pyrometer continuously measuring the sample temperature. The mixed metal oxides produced using

1 this system have been characterised in terms of their crystallinities, their specific surface areas, their  
2 basicities (concentrations and strengths of basic sites measured by carbon dioxide adsorption  
3 calorimetry), and their catalytic activities. The model reaction used has been the base-catalysed  
4 transesterification of glyceryl tributyrate with methanol (Scheme 1). This reaction is a mimic for the  
5 transesterification of vegetable oils used in biodiesel synthesis. From the point of view of catalyst  
6 testing, the use of glyceryl tributyrate has an advantage over vegetable oils in that it is fully miscible  
7 with methanol, meaning that it is easier to ensure that the transesterification reaction is carried out in  
8 the regime of kinetic rather than diffusion control.

9

10 *Scheme 1*

11

## 12 **2. Experimental**

13

### 14 *2.1. Catalyst preparation*

15 All reagents were of Analar grade. Metal nitrates were purchased from Sigma-Aldrich. A layered  
16 double hydroxide based on magnesium and aluminium (with an  $M^{2+}/M^{3+}$  ratio of 3.0) in which half  
17 the magnesium(II) in the synthesis mixture is substituted by copper(II) was prepared by adding slowly  
18 a 250 mL solution of magnesium, copper and aluminium nitrates, (total concentration  $1.00 \text{ mol dm}^{-3}$ ),  
19 to a 250 mL solution of sodium carbonate, ( $0.625 \text{ mol dm}^{-3}$ ) with stirring. The pH of the solution was  
20 maintained at 8-9 using sodium hydroxide solution ( $0.0200 \text{ mol dm}^{-3}$ ). The resulting mixture was  
21 aged at  $65 \text{ }^\circ\text{C}$  for two hours, cooled and filtered. The precipitate was washed thoroughly and dried at  
22  $100 \text{ }^\circ\text{C}$  overnight.

23

24 Powders, as 2.0 g samples, were calcined both conventionally in a muffle furnace in flowing dry air,  
25 and under feedback-controlled microwave heating at temperatures from  $400 \text{ }^\circ\text{C}$  to  $750 \text{ }^\circ\text{C}$  in flowing  
26 dry air, by heating at  $2 \text{ }^\circ\text{C min}^{-1}$  and then holding at the calcination temperature for four hours. All  
27 measurements refer to the calcined materials. Calcined samples were transferred to the reaction  
28 mixture in a desiccator.

1  
2  
3  
4  
5  
6  
7  
8  
9  
10  
11  
12  
13  
14  
15  
16  
17  
18  
19  
20  
21  
22  
23  
24  
25  
26  
27  
28

## 2.2. *Microwave calcination*

Samples were calcined in the microwave field in a single mode tuned cavity, using feedback-control to maintain the temperature ramp and a constant temperature in the isothermal region. In this system a variable power (to 1 kW) Industrial Microwave Systems microwave generator operating at 2.45 GHz through a Remote Head, feeds a wave guide with a three stub tuner. A resonant cavity accommodates the sample, positioned on a silica stub. The sample can be in the form of a pressed disc (or discs) or as a powder held in a silica crucible. The sample stub and sample are in a vertical silica sleeve through which a flow ( $5 \text{ mL min}^{-1}$ ) of dry air is maintained. Sample temperature is monitored using an Omega Engineering infrared pyrometer located a minimum distance above the sample cavity. The power is controlled using algorithms designed so that the sample follows a defined temperature, sample mass or evolved gas programme [8-10]. In the work reported here feedback was controlled to maintain a sample heating rate of  $2 \text{ }^\circ\text{C min}^{-1}$ , followed by an isothermal stage.

## 2.3. *Catalyst characterisation*

### 2.3.1. *XRD, $N_2$ adsorption and XPS*

Catalysts were stored in a dry atmosphere at room temperature. They were characterised by powder X-ray diffraction using  $\text{Cu K}\alpha$  radiation (Bruker AXS-D8 Advance Diffractometer) and by nitrogen adsorption at  $-196 \text{ }^\circ\text{C}$  (Micrometrics ASAP 2020) after degassing at  $150 \text{ }^\circ\text{C}$ , using 30 data points. Surface areas were determined from adsorption isotherms (BET). Exposure to air for oxide samples was minimised to prevent reaction with water vapour and conversion back to hydroxides. The close-to-surface elemental composition of the copper-substituted hydrotalcite was determined by X-ray photoelectron spectroscopy, at the Institut de Recherches sur la Catalyse et l'Environnement de Lyon.

### 2.3.2. *Calorimetric adsorption experiments*

Catalyst basicity was characterised by carbon dioxide adsorption calorimetry, under flow conditions, using a system based on a flow-through Setaram 111 differential scanning calorimeter (DSC) and an automated gas flow and switching system, with a mass spectrometer connected via a heated capillary (at  $175 \text{ }^\circ\text{C}$ ) for the down-stream gas flow detection [32,33]. In a typical experiment a sample ( $\sim 50$



1 mg) is activated under dry nitrogen ( $5 \text{ mL min}^{-1}$ ) for one hour at  $200 \text{ }^\circ\text{C}$ . It is then cooled to  $120 \text{ }^\circ\text{C}$   
2 and small pulses (typically  $1 \text{ mL}$ ) of the probe gas (1% carbon dioxide in nitrogen) are injected at  
3 regular intervals into the carrier gas stream from a gas sampling valve. The concentration of carbon  
4 dioxide ( $m/z - 44$ ) downstream of the sample is monitored. An important feature of the flow  
5 calorimetric technique is that net heat measurements relate only to carbon dioxide bound irreversibly  
6 to the samples. Reversibly bound carbon dioxide desorbs when the gas flow reverts to the carrier gas.  
7 The net amount of carbon dioxide irreversibly adsorbed from each pulse is determined by comparing  
8 the mass spectrometer signal during each pulse with a signal recorded during a control experiment  
9 through an empty sample tube. Net heat released for each pulse is calculated from the DSC thermal  
10 curve. From this the molar enthalpy of adsorption ( $\Delta H_{\text{ads}}^\circ$ ) is obtained for the carbon dioxide adsorbed  
11 from each pulse. In this work, each sample was analysed in triplicate under the same experimental  
12 conditions. Data is plotted as a profile of  $\Delta H_{\text{ads}}^\circ(\text{CO}_2)$  vs. amount of carbon dioxide irreversibly  
13 adsorbed.

14

#### 15 *2.4 Catalytic activities*

16 The catalytic activities of the oxides were determined in the transesterification of glyceryl tributyrate  
17 (tributylin) with methanol. Methanol ( $12.0 \text{ mL}$ , Sigma-Aldrich, purity 99.8%), internal standard  
18 dihexyl ether ( $0.5 \text{ mL}$ , Sigma-Aldrich) and glyceryl tributyrate ( $5.0 \text{ mL}$ , Sigma-Aldrich, purity  $\geq 99\%$ )  
19 were placed in a  $50 \text{ mL}$  three-necked round bottom flask with a condenser attached, and heated with  
20 stirring at  $250 \text{ rpm}$ , to  $65 \text{ }^\circ\text{C}$ . The catalyst ( $250 \text{ mg}$ ) was activated at  $150 \text{ }^\circ\text{C}$  for one hour prior to  
21 reaction and then added to the pre-heated reaction mixture. Conversion of tributyrin and product  
22 formation were monitored by GC, using a  $25 \text{ m BP1}$  column at  $1.4 \text{ mL min}^{-1}$  helium flow, split ratio  
23 28:1, at time zero and at regular intervals over a reaction period of three hours. Reaction rates were  
24 measured over a range of stirrer speeds to ensure that we were not operating in a diffusion control  
25 regime. Similarly, metal oxide powders were ground with a pestle and mortar under dry air and the  
26 reactions run again, to ensure that catalyst particle size was not affecting reaction rate. The possibility  
27 of catalyst leaching was eliminated by removing catalyst at an intermediate reactant conversion and  
28 confirming that the reaction ceased.

1

## 2 **3. Results and Discussion**

3

### 4 *3.1 Copper-containing hydrotalcite*

5 Elemental analysis by XPS indicated that the stoichiometry of the mixed hydroxide on which this  
6 study was based corresponded to  $\text{Cu}_{1.4}\text{Mg}_{4.4}\text{Al}_{2.2}(\text{CO}_3)_{1.1}(\text{OH})_{16}$ . Analysis by XPS is limited to  
7 regions close to the solid surface but there is no reason to suppose that the bulk composition would be  
8 significantly different. The powder X-ray diffraction pattern is shown in Figure 2 and is typical for a  
9 hydrotalcite-type material [15, 34, 35] and is not significantly different from the pattern detected by  
10 Kovanda et al. for a hydrotalcite with metal stoichiometry  $\text{Cu}_2\text{Mg}_2\text{Al}_2$ [36]. The unit cell parameters  
11 were obtained based on a 3R stacking sequence so the spacing  $d_{110}$  can be used to calculate the  $a$  unit  
12 cell parameter ( $a = 2d_{110}$ ) which is sensitive to the ionic radii of the metal ions in the structure.  
13 Magnesium(II) and copper(II) ions have very similar radii so we cannot reasonably expect to be able  
14 to confirm the presence of copper(II) from this, but the value for  $a$  of 0.306 nm is broadly consistent  
15 with the composition, particularly the aluminium content, of the material [16]. The  $c$  parameter ( $c =$   
16  $3d_{003}$ ) is 2.33 nm for  $\text{Cu}_{1.4}\text{Mg}_{4.4}\text{Al}_{2.2}(\text{CO}_3)_{1.1}(\text{OH})_{16}$ . The value of this spacing is sensitive to the level  
17 of hydration but in this case is generally consistent with values detected for similar materials [16].

18

19

*Figure 2*

20

### 21 *3.2 Calcination conditions and effects on catalyst properties*

#### 22 *3.2.1 Products of calcination*

23 The material was calcined in a conventional furnace and in the microwave cavity under temperature  
24 feedback-control to final temperatures up to 750 °C. Diffraction patterns recorded after calcination at  
25 400, 500 and 750 °C are shown in Figure 3. Specific surface areas by nitrogen adsorption are shown  
26 in Table 1. Catalytic activities are also shown in the Table, in terms of the % conversions of glyceryl  
27 butyrate after 150 minutes reaction time. Conversion of glyceryl butyrate was monitored throughout

1 the reaction in all cases and the measured rates were essentially first order in this reactant (methanol  
2 was in large excess).

3

4 *Figure 3*

5

6 Figure 3 shows that, on calcination using both methods of heating, the material loses the hydrotalcite  
7 structure, and broad overlapping reflections due to MgO [37] and CuO [38] appear. As the  
8 temperature is increased further, the CuO reflections abruptly sharpen, clearly seen in the XRD  
9 pattern taken after microwave heating to 500 °C, followed by a similar sudden reduction in peak width  
10 for MgO, visible in the 750 °C microwave pattern but detected first at 550 °C (this XRD pattern is not  
11 shown). As heating continues reflections assigned to spinel, MgAl<sub>2</sub>O<sub>4</sub> [39], appear under both types  
12 of heating. In fact, these could be due to a copper-containing spinel [25], the diffraction pattern for  
13 which may be indistinguishable from that of MgAl<sub>2</sub>O<sub>4</sub>.

14

15 The diffraction patterns of MgO and CuO sharpen very abruptly during the heating process, implying  
16 that sintering of the small oxide crystallites responsible for the broad line patterns occurs quite  
17 suddenly. In general, material heated using microwaves exhibits more intense and better resolved  
18 lines for CuO, MgO and for spinel, suggesting that greater crystallinity is achieved using microwave  
19 heating. Furthermore, the appearance of these phases occurs at nominally slightly lower  
20 temperatures under microwave heating, clearly seen by comparing XRD patterns taken after heating  
21 to 500 °C under the two heating regimes.

22

23 *Figure 4*

24

25 At higher temperatures, illustrated by the results at 750 °C in Figure 3, the spinel phase is clearly  
26 visible, but an additional phase is also seen at this temperature when microwaves are used.  
27 Reflections in the 750 °C microwave diffraction pattern are assigned in Figure 4 and the reflections  
28 associated with this new phase can be matched to those of Cu<sub>2</sub>MgO<sub>3</sub>, gueggonite, which has been

1 detected by others on heating simple solid mixtures of CuO and MgO in a conventional furnace to  
2 1000 °C [40]. It has also been detected by X-ray diffraction in a copper-containing hydrotalcite of  
3 nominal stoichiometry  $\text{Cu}_2\text{Mg}_2\text{Al}_2(\text{CO}_3)(\text{OH})_{12}$  following calcination at 1000 °C, with reflections  
4 becoming quite intense at 1100 °C [36]. While we detected this phase at 750 °C under microwave  
5 heating, we could find no evidence for it when  $\text{Cu}_{1.5}\text{Mg}_{4.5}\text{Al}_2(\text{CO}_3)(\text{OH})_{16}\cdot 4\text{H}_2\text{O}$  was calcined under  
6 conventional heating, even to 1100 °C, despite the existence of a CuO/MgO mixture at temperatures  
7 above 500 °C. The relatively low copper content of the materials we have worked with is probably  
8 responsible for the absence of evidence for  $\text{Cu}_2\text{MgO}_3$  on conventional calcination. The contrasting  
9 clear detection of  $\text{Cu}_2\text{MgO}_3$  diffraction lines on microwave heating suggests the phase is formed  
10 relatively easily under this form of heating. Why this difference should exist is unclear but it does  
11 suggest that the processes induced by microwave heating are not the same as by conventional heating.

12

13 *Table 1*

14

15 There are small differences in the way the specific surface areas of the calcined materials change with  
16 calcination temperature, shown in Table 1. It is significant that specific surface areas go through  
17 maxima under both heating regimes, with materials calcined at 750 °C showing relatively low surface  
18 areas. Catalytic activities, on the other hand, increase with calcination temperature right through to  
19 750 °C. Significantly, microwave calcined oxides show consistently higher activities than their  
20 conventionally calcined counterparts, despite the fact that their surface areas are generally lower.  
21 Analysis of the products of the transesterification show that selectivity to methyl butanoate at 2.5  
22 hours reaction time is between 55 and 70%, and the patterns of selectivity are the same for the  
23 catalysts prepared in the two ways. The other products are the intermediate diglyceride and  
24 monoglyceride, and in all cases these are converted to the methyl ester completely as the reaction  
25 proceeds. The measured selectivities are consistent with the findings of other workers who used other  
26 calcined layered double hydroxide catalysts for the same reaction [12].

27

28 *3.2.2 Catalyst basicities*

1 Calorimetric CO<sub>2</sub> adsorption data for material calcined at 400, 500 and 750 °C is shown in Figure 5,  
2 in which  $\Delta H^{\circ}_{\text{ads}}(\text{CO}_2)$  is plotted against the amount of CO<sub>2</sub> adsorbed by the sample. Catalyst  
3 basicities can be compared using these profiles, taking note of the extent of irreversible CO<sub>2</sub>  
4 adsorption with enthalpies greater than an arbitrary threshold of 60 kJ mol<sup>-1</sup>, below which adsorption  
5 can reasonably be considered to be on sites of insignificantly low base strength. Other workers have  
6 used similar thresholds for this [11]. The molar enthalpies of CO<sub>2</sub> adsorption reflect the strengths of  
7 basic sites on which the probe gas is adsorbed, so the profiles shown in Figure 5 can loosely be  
8 interpreted in terms of basic site strength distribution profiles.

9  
10 *Figure 5*

11  
12 The profiles exhibited by mixed oxides generated by the two methods of heating are very different.  
13 Conventionally calcined materials at 400 and 500 °C show relatively few basic sites and relatively low  
14 base strengths (the first pulses of CO<sub>2</sub> adsorb at only 100-110 kJ mol<sup>-1</sup>). The oxide produced at 750  
15 °C shows stronger sites; the first pulse adsorbs at 133 kJ mol<sup>-1</sup>. This material exhibits a higher  
16 concentration of basic sites at ca. 0.06 mmol g<sup>-1</sup> based on the 60 kJ mol<sup>-1</sup> cut-off. In contrast, the  
17 oxides produced by microwave calcination at 400, 500 and 750 °C show relatively strong base sites,  
18 with a significant part of the profiles in Figure 5b being above 120 k mol<sup>-1</sup>. The concentrations of  
19 basic sites on these materials are much higher at 0.13-0.15 mmol g<sup>-1</sup>, and the concentrations change  
20 relatively little over the calcination temperature range. It appears that surface basicity is generated by  
21 microwave heating much more effectively and at considerably lower temperatures than by  
22 conventional heating, both in terms of the concentrations of sites and site strengths.

23  
24 Overall, the results show that there are significant differences between the products of calcination  
25 under the two modes of heating. The relative rates at which CuO and MgO are formed under  
26 microwave heating and the rates of subsequent conversions to spinel are significantly different to  
27 those observed under conventional heating, and material prepared using microwaves are more  
28 crystalline and have somewhat lower surface areas than materials calcined conventionally. In

1 addition, microwave heating appears to facilitate the formation of the additional phase,  $\text{Cu}_2\text{MgO}_3$ .  
2 Catalysts prepared using microwaves show higher surface basicities (concentrations and strengths of  
3 basic sites) and, consistent with this, higher catalytic activities in a base-catalysed reaction, although  
4 differences in catalytic activities are not as great as might be expected based on  $\text{CO}_2$  calorimetric  
5 adsorption data. In fact, catalysts calcined at  $400\text{ }^\circ\text{C}$  by both methods of heating show similar  
6 activities, despite the dramatic differences in both the concentration and strength of basic sites  
7 measured calorimetrically. At the two higher calcination temperatures, microwave-calcined catalysts  
8 are significantly more active, but these differences do not appear to correlate directly with either the  
9 abundance or the strength of basic sites. Values for base site turnover frequencies (TOF) would have  
10 been useful in explaining differences in catalytic activities but, because we have used a rather  
11 arbitrary threshold of  $\text{CO}_2$  molar adsorption enthalpy on which to base our estimates of relative base  
12 site concentrations, we cannot calculate TOF values with any reliability. It seems likely to us that  
13 other factors, particularly pore structure and pore size, influence catalytic activity and, overall, it is  
14 not surprising that surface basicity alone is not a very good predictor of activity.

15  
16 Some of these differences between catalysts prepared in the two ways may be linked to the different  
17 temperature gradients developed in solid samples as they are heated in a microwave field, and the  
18 relative rates at which dehydration, dehydroxylation and decarbonation occur in the bulk and near the  
19 surface of the solid. It is not unreasonable to suppose that the structural disruption, and the different  
20 water vapour pressures and  $\text{CO}_2$  partial pressures to which regions of the sample would be exposed,  
21 could affect the conversion of one phase to another as the temperature is increased. However, the  
22 way in which surface basicity is developed so effectively under microwave heating suggests that this  
23 form of heating somehow facilitates the dehydroxylation step that generates the basic sites. It is  
24 possible that, as dehydroxylation occurs, the water released by the process is more susceptible to  
25 microwave heating than the rest of the solid. In this way, highly localised temperature excursions  
26 which are not affecting the bulk temperature significantly might occur, and it is possible that these  
27 high temperatures around the sites of oxide formation give rise to, firstly, highly effective

1 dehydroxylation and, secondly, the formation of surface defects and surface basicity as a consequence  
2 of very high local reaction rates.

3  
4 The idea that microwave heating might produce highly localised hot spots, possibly as water is  
5 released from the lattice, might also explain the formation of  $\text{Cu}_2\text{MgO}_3$ . We suggest that the reason  
6 we do not detect this phase under conventional heating is that the copper content of the hydrotalcite  
7 we have worked with is relatively low and, even at  $1100\text{ }^\circ\text{C}$ , aggregation of sufficient copper ions to  
8 form detectable levels of  $\text{Cu}_2\text{MgO}_3$  is not possible. But when microwave heating is employed,  
9 localised temperatures far in excess of this may be developed, facilitating aggregation and the  
10 formation of easily detectable levels of  $\text{Cu}_2\text{MgO}_3$ .

11  
12 We suggest that microwave-induced processes, even when under control at a bulk sample level, may  
13 produce very large temperature differences within a solid material at a highly localised level.

14 If this is the case, and if temperatures far in excess of the bulk temperature are being experienced  
15 locally, then processes that would not normally be considered possible may need to be taken into  
16 account. In the case of hydrotalcites, the decomposition of carbonate ions is, in general, considered  
17 to be almost complete below  $400\text{ }^\circ\text{C}$ , but in fact it is known that complete decarbonation requires  
18 much higher temperatures, up to  $800\text{ }^\circ\text{C}$  [26]. There is infrared spectral evidence for a small  
19 proportion of the carbonate ions in the interlayer region becoming chemically grafted to the layered  
20 hydroxide, and it is likely that it is these grafted carbonate ions that decompose only at high  
21 temperatures [41]. It is conceivable that these grafted, thermally stable, carbonate ions remain intact  
22 on conventional calcination but are decomposed on microwave heating. And a possibility is that it is  
23 the complete removal of these interlayer carbonate ions that is required in order to generate the mixed  
24 metal oxides with maximised surface basicity.

25  
26 To understand this further, it will be helpful to study hydrotalcites with other metals substituted for  
27 magnesium. Copper-containing hydrotalcites are generally thought to show lower basicities than  
28 hydrotalcites containing many other substituent metals, including lanthanum [42] and nickel [43], and

1 current work is directed towards hydrotalcites containing these other metals, with the objective of  
2 identifying the role of the transition metal substituent in the development of basicity under different  
3 modes of calcination.

4

#### 5 **4. Conclusion**

6

7 The concentrations and strengths of basic sites on calcined  $\text{Cu}_{1.4}\text{Mg}_{4.4}\text{Al}_{2.2}(\text{CO}_3)_{1.1}(\text{OH})_{16}$  are  
8 significantly higher when the hydrotalcite is calcined using microwaves, under feedback-control, than  
9 when using conventional heating. As would be predicted, this translates into higher catalytic activity  
10 in a base-catalysed reaction. It seems likely that, even when the microwave heating process is  
11 controlled via the bulk temperature of the solid, very high localised temperatures might be responsible  
12 for the formation of high concentrations of relatively strong basic surface sites.

13

14 We therefore believe that this work illustrates the value of feedback-controlled microwave heating for  
15 the conversion of hydroxides to metal oxid catalysts. The control ensures that bulk temperature  
16 runaway does not occur but, at the same time, allows for the sometimes beneficial local temperature  
17 excursions brought about by microwaves which can lead to increased surface basicity and catalytic  
18 activity.

19

#### 20 **4. Acknowledgements**

21

22 The University of Huddersfield is thanked for a studentship (HEC). Thanks are due to Professor A  
23 Auroux of the Institut de Recherches sur la Catalyse et l'Environnement de Lyon (IRCELYON) for  
24 providing XPS measurements.

25

#### 26 **5. References**



- 1 [1] A. Harrison, R. Ibberson, G. Robb, G. Whittaker, C. Wilson, I.D. Youngson, *Faraday*  
2 *Discuss.* 122 (2002) 363-399.
- 3 [2] D.R. Baghurst, R.C.B. Copley, H. Fleischer, D.M.P. Mingos, G.O. Kyd, L.J. Yellowlees, A.J.  
4 Welch, T.R. Spalding, D. O'Connell, *J Organomet. Chem.* 447 (1993) C14-C17.
- 5 [3] A.G. Whittaker, A. Harrison, G.S. Oakley, I.D. Youngson, S. King, R. Heenan, *Rev. Sci.*  
6 *Instrum.* 72 (2001) 172-176.
- 7 [4] M. Willert-Porada, *Ceram. Trans.* 80 (1997) 153-163.
- 8 [5] J.H. Booske, R.F. Cooper, I. Dobson, *J. Mater. Res.* 7 (1992) 495-501.
- 9 [6] J.H. Booske, R.F. Cooper, S.A. Freeman, K.I. Rybakov, V.E. Semenov, *Phys. Plasmas*, 5  
10 (1998) 1664-1670.
- 11 [7] S.A. Freeman, J.H. Booske, R.F. Cooper, *J. Appl. Phys.* 83 (1998) 5761-5772.
- 12 [8] E.A. Fesenko, P.A. Barnes, G.M.B. Parkes, in: *Sample Controlled Thermal Analysis. Hot*  
13 *Topics in Thermal Analysis and Calorimetry*, 3 (Eds: O.T. Sorensen, J. Rouquerol) Springer:  
14 New York, 2004, pp.174-225.
- 15 [9] P.A. Barnes, E.L. Charsley, G.M.B. Parkes, *Eur. Pharm. Rev.* 11 (2006) 83-98.
- 16 [10] B.K.N.S. Kumar, G.M.B. Parkes, P.A. Barnes, M.J.N. Sibley, G. Bond, *Rev. Sci. Instrum.*  
17 77 (2006) 045108/1-145108/9.
- 18 [11] H.A. Prescott, Z-L. Li, E. Kemnitz, A. Trunschke, J. Deutsch, H. Lieske, A. Auroux, *J. Catal.*  
19 234 (2005) 119-130.
- 20 [12] J.L. Shumaker, C. Crofcheck, S.A. Tackett, E. Santillan-Jimenez, T. Morgan, Y. Ji, M.  
21 Crocker, T.J. Toops, *Appl. Catal. B* 82 (2008) 120-130.

- 1 [13] J.S. Valente, F. Figueras, M. Gravelle, P. Kumbhar, J. Lopez, J-P. Besse, *J. Catal.* 189 (2000)  
2 370-381.
- 3 [14] D.G. Cantrell, L.J. Gillie, A.F. Lee, K. Wilson, *Appl. Catal. A* 287 (2005) 183-190.
- 4 [15] F. Figueras, *Topics in Catal.* 29 (2004) 189-196.
- 5 [16] J.S. Valente, J. Hernandez-Cortez, M.S. Cantu, G. Ferrat, E. Lopez-Salinas, *Catal. Today* 150  
6 (2010) 340-345.
- 7 [17] I-C. Marcu, D. Tichit, F. Fajula, N. Tanchoux, *Catal. Today* 147 (2009) 231-238.
- 8 [18] D. Meloni, R. Monaci, V. Solinas, A. Auroux, E. Dimitriu, *Appl. Catal. A* 350 (2008) 86-95.
- 9 [19] L. Dussault, J.C. Dupin, E. Dumitriu, A. Auroux, C. Guimon, *Surface & Interface Anal.* 38  
10 (2006) 234-237.
- 11 [20] A. Venugopal, J. Palgunadi, J-K. Deog, O-S. Joo, C-H. Shin, *Catal. Today* 147 (2009) 94-99.
- 12 [21] J.J. Yu, J. Cheng, C.Y. Ma, H.L. Wang, H.D. Li, Z.P. Hao, Z.P. Xu, *J. Colloid and Interface*  
13 *Sci.* 333 (2009) 423-430.
- 14 [22] M. Sanchez-Cantu, L.M. Perez-Diaz, A.M. Maubert, J.S. Valente, *Catal. Today* 150 (2010)  
15 332-339.
- 16 [23] W. Zhongpeng, J. Zhi, S. Wenfeng, *Catal. Commun.* 8 (2007) 1659-1664.
- 17 [24] M.J. Hudson, S. Carlino, D.C. Apperley, *J. Mater. Chem.* 5 (1995) 323-329.
- 18 [25] S. Kannan, V. Rives, H. Knozinger, *J. Solid State Chem.* 117 (2004) 319-331.
- 19 [26] J.T. Klopogge, L. Hickey, R.L. Frost, *Appl. Clay Sci.* 18 (2001) 37-49.
- 20 [27] R. Trujillano, M.J. Holgado, V. Rives, *Solid State Science* 11 (2009) 688-693.
- 21 [28] V. Vagvolgyi, A. Locke, M. Hales, J. Kristof, R.L. Frost, E. Horvath, W.N. Martens,  
22 *Thermochim. Acta* 468 (2008) 81-86.

- 1 [29] V. Vagvolgyi, S.J. Palmer, J. Kristof, R.L. Frost, E. Horvath, *J. Colloid and Interface Sci.* 318  
2 (2008) 302-308.
- 3 [30] M.M. Amini, L. Torkian, *Mater. Lett.* 57 (2002) 639-642.
- 4 [31] M. Willert-Porada, T. Krummel, B. Rhohe, D. Moorman, *Mater. Res. Soc. Symp. Proc.* 269  
5 (1992) 199-206.
- 6 [32] N.R. Shiju, H.M. Williams, D.R. Brown, *Appl. Catal. B* 90 (2009) 451-457.
- 7 [33] P.F. Siril, N.R. Shiju, D.R. Brown, K. Wilson, *Appl. Catal. A* 364 (2009) 95-100.
- 8 [34] J. Shen, J.M. Kobe, Y. Chen, J.A. Dumesic, *Langmuir* 10 (1994) 3902-3908.
- 9 [35] J. Rocha, M. del Arco, M.A. Ulibarri, *J. Mater. Chem.* 9 (1999) 2499-2503.
- 10 [36] F. Kovanda, K. Jiratova, J. Rymes, D. Kolousek, *Appl. Clay Sci.* 18 (2001) 71-80.
- 11 [37] JCPDS Card 4-829 Intl. Centre for Diffraction Data 1987.
- 12 [38] H. Wang, J-Z Xu, J-J Zhu, H-Y Chen, *J. Crystal Growth* 244 (2002) 88-94.  
13  
14
- 15 [39] JCPDS Card 21-1152 Intl. Centre for Diffraction Data 1987.
- 16 [40] H.G. El-Shobaky, *J. Therm. Anal & Calor.* 85 (2006) 32-327.
- 17 [41] T. Stanimirova, I. Veriglov, G. Kirov, N. Petrova, *J. Mater. Sci.* 34 (1999) 4153-4161.
- 18 [42] B. Veldurihy, J-M. Clacens, F. Figueras, *J. Catal.* 229 (2005) 237-242.
- 19 [43] C. Casenave, H. Martinez, C. Guimon, A. Auroux, A. Cordoneanu, E. Dumitriu, *Thermochim*  
20 *Acta* 379 (2001) 85-93.
- 21

1 **Figure captions**

2

3 Fig. 1. Temperature and power vs time plots for a copper(II)-containing hydrotalcite under microwave  
4 heating, a) where microwave power is increased linearly with time, showing sample temperature  
5 fluctuations and temperature runaway, and b) where the power is controlled to give a linear  
6 temperature increase.

7

8

9 Fig. 2. Powder XRD pattern of  $\text{Cu}_{1.4}\text{Mg}_{4.4}\text{Al}_{2.2}(\text{CO}_3)_{1.1}(\text{OH})_{16}$ .

10

11 Fig. 3. Powder X-ray diffraction patterns for  $\text{Cu}_{1.4}\text{Mg}_{4.4}\text{Al}_{2.2}(\text{CO}_3)_{1.1}(\text{OH})_{16}$  following: a) conventional  
12 and b) microwave calcination, to the temperatures indicated.

13

14 Fig. 4. Powder X-ray diffraction pattern for  $\text{Cu}_{1.4}\text{Mg}_{4.4}\text{Al}_{2.2}(\text{CO}_3)_{1.1}(\text{OH})_{16}$  following calcinations  
15 under microwave heating at 750 °C.

16

17 Fig. 5. Differential molar enthalpies of  $\text{CO}_2$  adsorption vs. amount of  $\text{CO}_2$  adsorbed at 120 °C  
18 for  $\text{Cu}_{1.4}\text{Mg}_{4.4}\text{Al}_{2.2}(\text{CO}_3)_{1.1}(\text{OH})_{16}$  following calcination at 400, 500 and 750 °C under a)  
19 conventional and b) microwave heating.

20

21 **Table caption**

22

23 Table 1. Specific surface areas (BET) and catalytic activities of  $\text{Cu}_{1.4}\text{Mg}_{4.4}\text{Al}_{2.2}(\text{CO}_3)_{1.1}(\text{OH})_{16}$   
24 following conventional (furnace) calcination and feedback-controlled microwave calcination.

25

Table 1

Specific surface areas (BET) and catalytic activities of  $\text{Cu}_{1.4}\text{Mg}_{4.4}\text{Al}_{2.2}(\text{CO}_3)_{1.1}(\text{OH})_{1.6}$  following conventional (furnace) calcination and feedback-controlled microwave calcination.

Calcination temperature /°C	Conventional heating			Controlled microwave heating		
	Surface area /m <sup>2</sup> g <sup>-1</sup>	Catalytic activity <sup>a,b,c</sup> /conversion of tributyrin after 2.5 hours /%	Product selectivity to methyl butanoate <sup>d</sup> /%	Surface area /m <sup>2</sup> g <sup>-1</sup>	Catalytic activity <sup>a,b,c</sup> conversion of tributyrin after 2.5 hours /%	Product selectivity to methyl butanoate <sup>d</sup> /%
-	60	0	-	60	0	-
400	88	20	55	86	21	58
500	101	26	61	84	34	64
750	59	33	63	21	46	68

<sup>a</sup> Methanol 12.0 mL; glyceryl butyrate 5.0 mL; catalyst 250 mg; reaction temperature 65 °C.

<sup>b</sup> Conversion vs. time data appears in Supplementary Data (ESI).

<sup>c</sup> 95% confidence limits = ±3%.

<sup>d</sup> 95% confidence limits = ±5%.

FIGURE 1

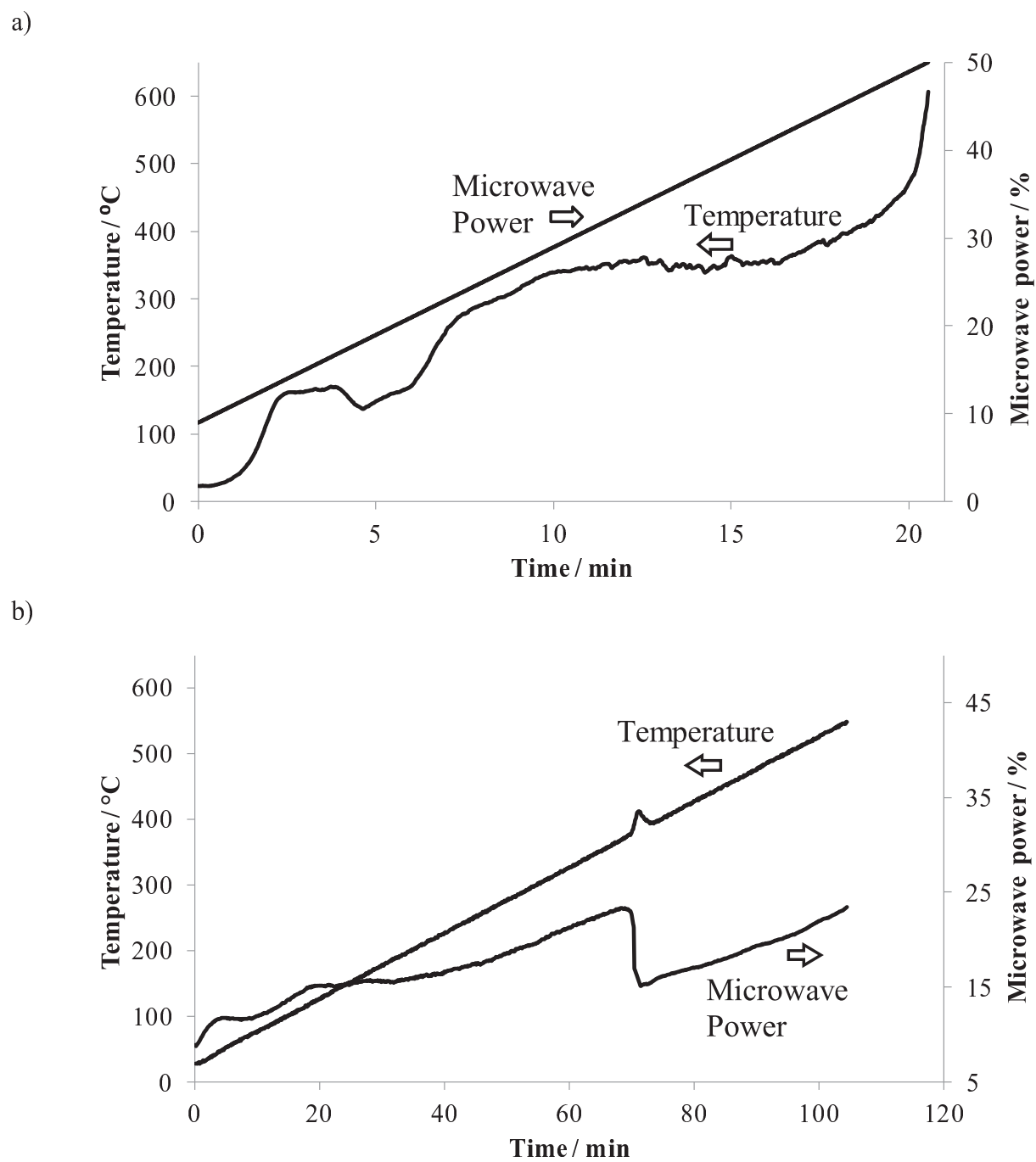


Fig. 1. Temperature and power vs time plots for a copper(II)-containing hydrotalcite under microwave heating, a) where microwave power is increased linearly with time, showing sample temperature fluctuations and temperature runaway, and b) where the power is controlled to give a linear temperature increase.

SCHEME 1

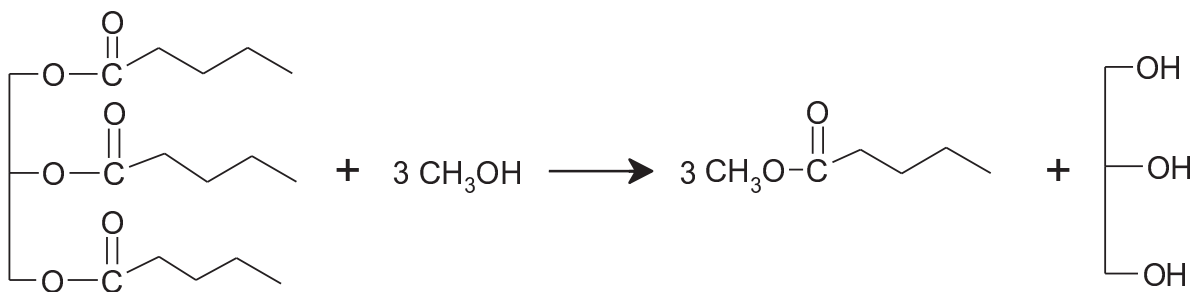


FIGURE 2

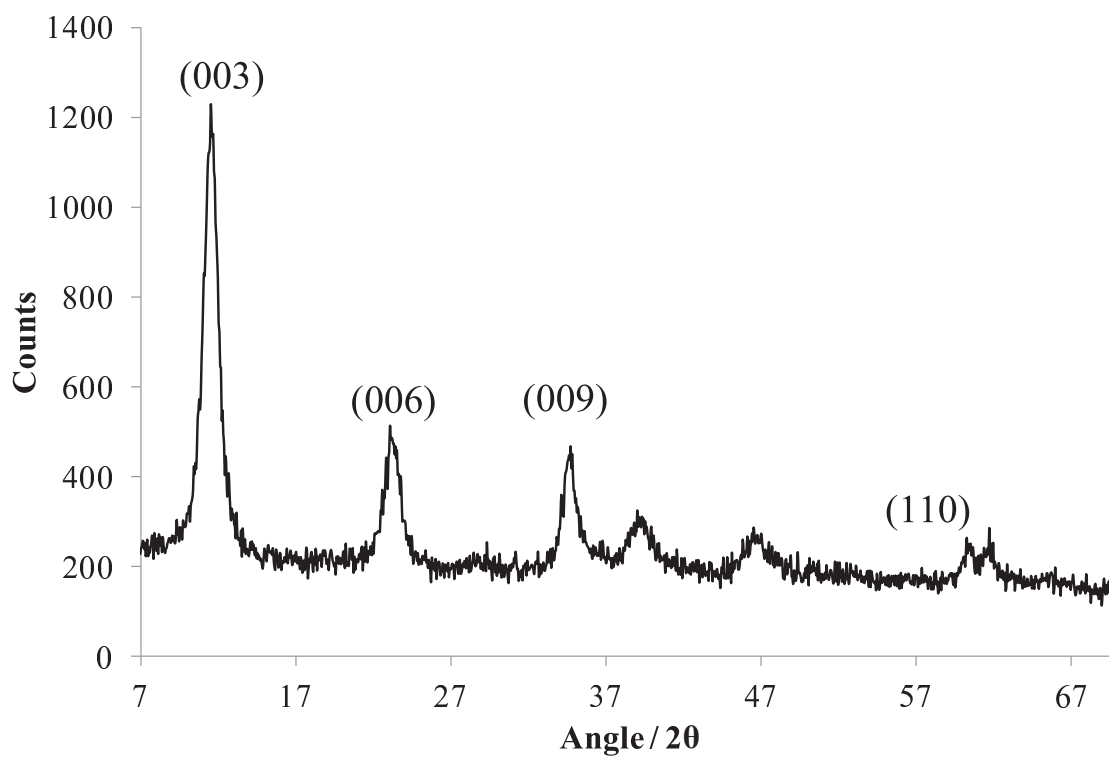
Fig. 2. Powder XRD pattern of  $\text{Cu}_{1.4}\text{Mg}_{4.4}\text{Al}_{2.2}(\text{CO}_3)_{1.1}(\text{OH})_{16}$ .



FIGURE 3

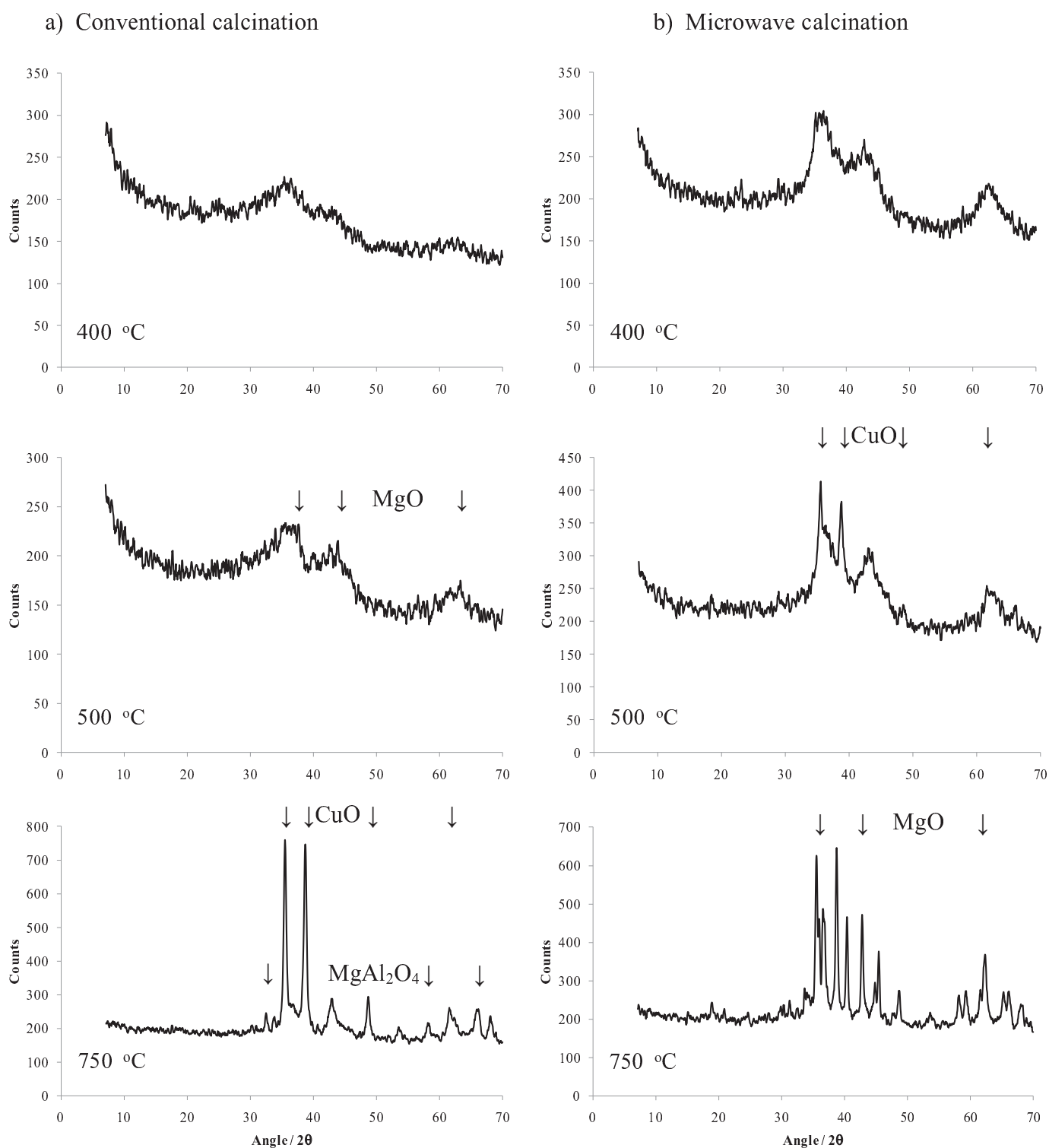


Fig. 3. Powder X-ray diffraction patterns for  $\text{Cu}_{1.4}\text{Mg}_{4.4}\text{Al}_{2.2}(\text{CO}_3)_{1.1}(\text{OH})_{16}$  following: a) conventional and b) microwave calcination, to the temperatures indicated.

FIGURE 4

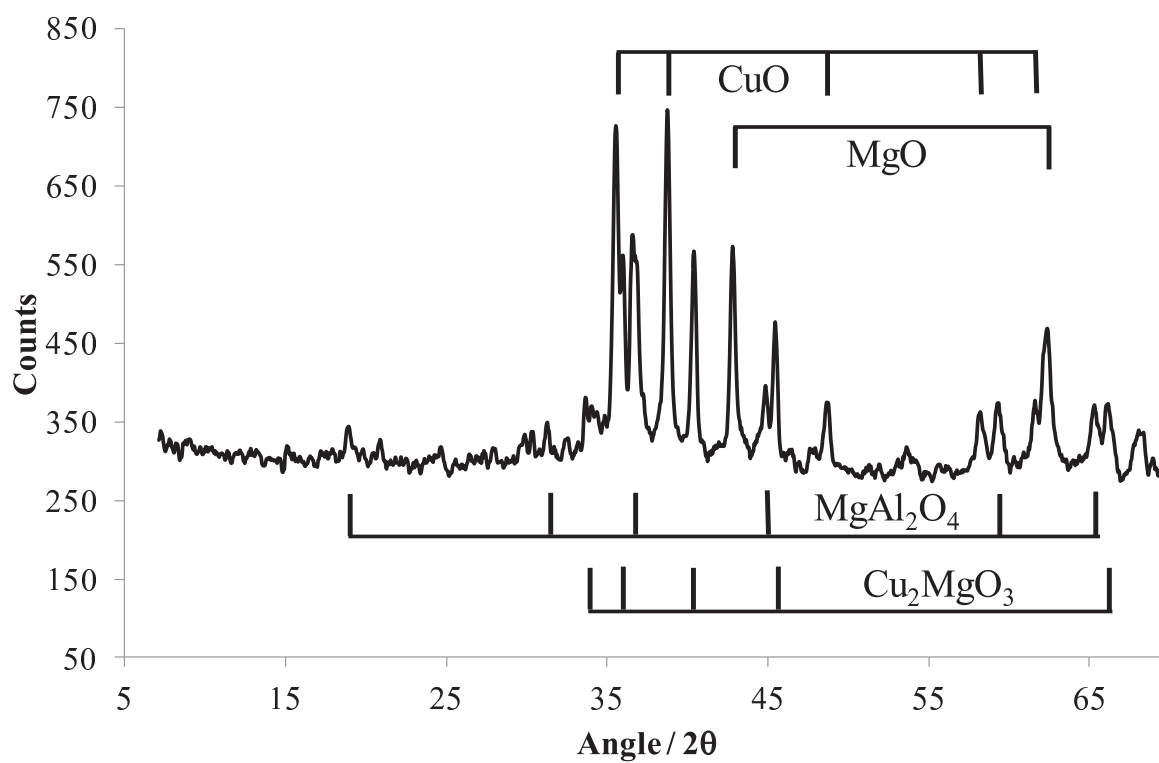
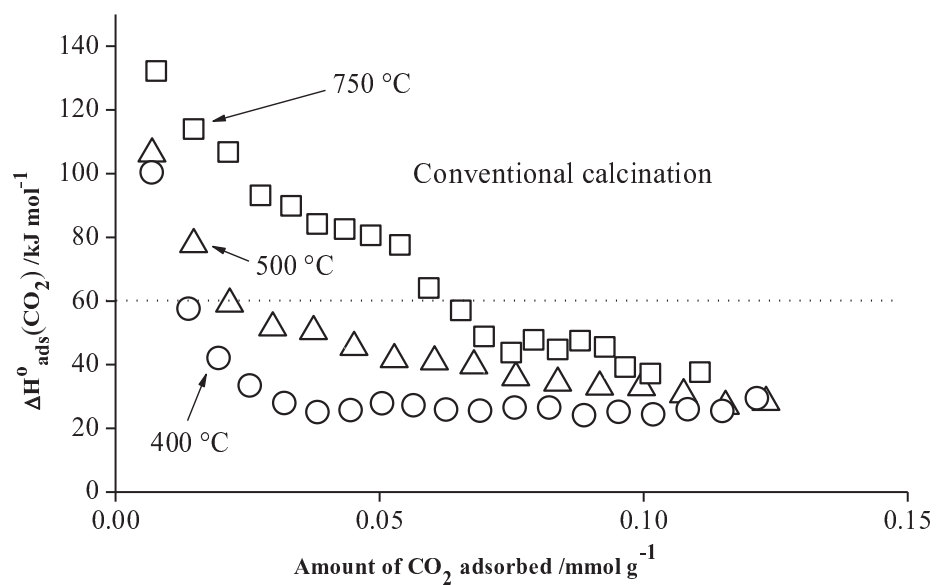


Fig. 4. Powder X-ray diffraction pattern for  $\text{Cu}_{1.4}\text{Mg}_{4.4}\text{Al}_{2.2}(\text{CO}_3)_{1.1}(\text{OH})_{16}$  following calcinations under microwave heating at  $750\text{ }^\circ\text{C}$ .

FIGURE 5

a)



b)

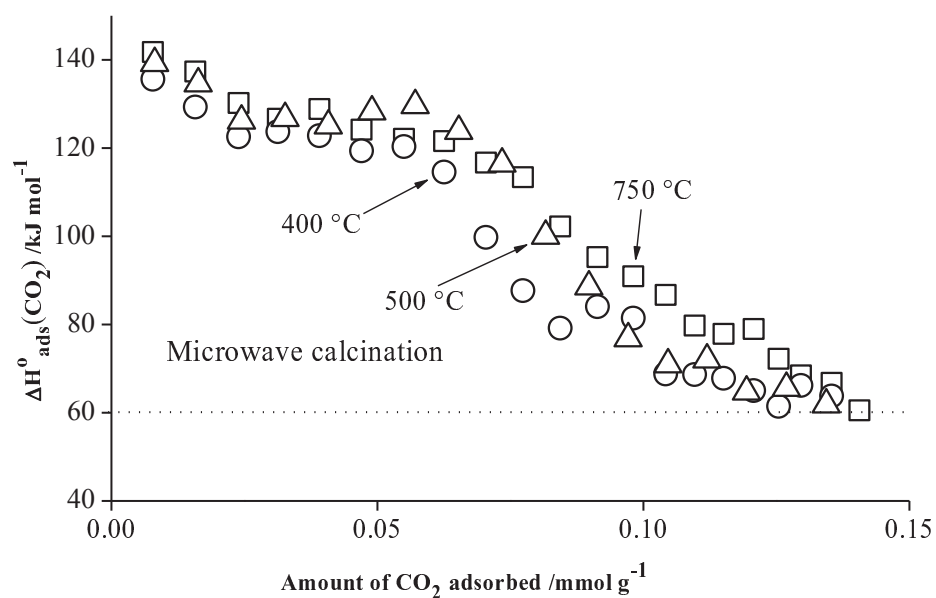


Fig. 5. Differential molar enthalpies of  $\text{CO}_2$  adsorption vs. amount of  $\text{CO}_2$  adsorbed at 120 °C for  $\text{Cu}_{1.4}\text{Mg}_{4.4}\text{Al}_{2.2}(\text{CO}_3)_{1.1}(\text{OH})_{16}$  following calcination at 400, 500 and 750 °C under a) conventional and b) microwave heating.

### Figure captions

Fig. 1. Temperature and power vs time plots for a copper(II)-containing hydrotalcite under microwave heating, a) where microwave power is increased linearly with time, showing sample temperature fluctuations and temperature runaway, and b) where the power is controlled to give a linear temperature increase.

Fig. 2. Powder XRD pattern of  $\text{Cu}_{1.4}\text{Mg}_{4.4}\text{Al}_{2.2}(\text{CO}_3)_{1.1}(\text{OH})_{16}$ .

Fig. 3. Powder X-ray diffraction patterns for  $\text{Cu}_{1.4}\text{Mg}_{4.4}\text{Al}_{2.2}(\text{CO}_3)_{1.1}(\text{OH})_{16}$  following: a) conventional and b) microwave calcination, to the temperatures indicated.

Fig. 4. Powder X-ray diffraction pattern for  $\text{Cu}_{1.4}\text{Mg}_{4.4}\text{Al}_{2.2}(\text{CO}_3)_{1.1}(\text{OH})_{16}$  following calcinations under microwave heating at 750 °C.

Fig. 5. Differential molar enthalpies of  $\text{CO}_2$  adsorption vs. amount of  $\text{CO}_2$  adsorbed at 120 °C for  $\text{Cu}_{1.4}\text{Mg}_{4.4}\text{Al}_{2.2}(\text{CO}_3)_{1.1}(\text{OH})_{16}$  following calcination at 400, 500 and 750 °C under a) conventional and b) microwave heating.

### Table caption

Table 1. Specific surface areas (BET) and catalytic activities of  $\text{Cu}_{1.4}\text{Mg}_{4.4}\text{Al}_{2.2}(\text{CO}_3)_{1.1}(\text{OH})_{16}$  following conventional (furnace) calcination and feedback-controlled microwave calcination.

**Supplementary Material**

[Click here to download Supplementary Material: supplementary 30Mar2012.doc](#)